Fundamental Studies of Linting: Understanding Ink-Press-Paper Interactions Non-Linearity

Patrice J. Mangin* and Jacques Silvy**

Keywords - Paper, lint, model, mechanism, printing, speed, pressure, ink

Abstract

The linting propensity of paper is the tendency of paper to shed loosely bonded surface fibres in offset printing. A model based on three forces that describe the complex interactions between ink, the paper surface, and the press conditions that create linting is briefly presented. Two forces are related to free and porous ink flow in the printing nip, and the third one is based on ink filament elongation after the printing nip. The model fully explains the synergy between printing pressure, press speed, ink viscosity, paper roughness, and pulp furnish mix. Results from printing on Dynamic Sheet Former samples are detailed. Due to the non-linearity and the synergy between linting and the various parameters, it is shown how, with the right combination, a low printing pressure can produce more lint than a high printing pressure, that a low viscosity ink can produce more lint than a higher viscosity, higher tack ink, and that, at low ink level, low printing speed can produce more lint than a higher printing speed. It is also shown that the speed effect is related to a threshold resistance of the paper surface to fibre removal. By comparison, the paper roughness and the pulp furnish have less effect on linting than the press parameters.

* Professor, Stora Chair, Royal Institute of Technology (KTH), Stockholm, Sweden
** Professor, Ecole Française de Papeterie et des Industries Graphiques de Grenoble (EFPG), Grenoble, France

Introduction

Linting is defined as the tendency of paper surfaces to shed loosely bonded surface fibres during offset printing. Not only does linting cause a deterioration in print quality but it is also the source of pressroom runnability problems. Accordingly, many tests have been designed to measure linting (Mangin 1987) with little understanding of the linting mechanisms. Theories of linting are many but none was found to properly describe the effect of press parameters (Mangin 1990a, 1991). Attempts to modify existing theories have stressed the need for a fundamental evaluation and understanding of the linting mechanisms (Mangin, Silvy, De Grâce, 1990) but concluded that no existing theory would explain the full fibre removal curve as a function of the ink weight on the printing plate. The first sign of a breakthrough was presented by Mangin and Silvy during the 1990 International Paper Physics seminar, based on previous work by Mangin (1988). Based on examination of the fibre removal curve, we then concluded that at least 3 forces were required to fully describe such behaviour. The variations of the amount of fibre removed during printing, expressed in unit length per unit area of paper, as a function of the ink weight on the printing plate before printing is shown in **Figure 1** for a rough uncalendered newsprint. Such curves, shown for printing speeds of 3.0, 4.6, and 6.0 m/s are called "fibre removal curves". The amount of lint removed from the paper surface can be seen to decrease rapidly at low ink weights, usually below 1.5-2.0 g/m2, then to increase, usually in the 5 to 20-25 g/m2 range. Of course, such a curve is theoretical as commercial printing ranges are below 5 g/m2. Unfortunately, in the region of interest, 1-5 g/m2, the curve behaviour is very complex and can sometimes take the shape of a "W". Such a complex curve shape was noticed by Oittinen (1976) in her PhD thesis but with no explanations. The decrease in lint removal at very high ink weights that could be predicted by the modified Stefan's law (Mangin, Silvy, De Grâce, 1990) only occurs when the paper is saturated with ink, i.e. for smooth, non-porous papers or papers where the surface is "closed". In such a situation a true splitting in a liquid phase occurs. This can be seen in **Figure 2** where the newsprint has been calendered to a Parker Print-Surf (PPS) roughness S10 (using the soft backing) value of 3.0 μm. Calendering has here closed the paper surface to ink penetration so that saturation in ink occurs in the printing nip. Description of such fibre removal curves required a new theory presented below. However, in the scope of this article, we will only focus on the effect of ink viscosity, printing speed, and printing pressure in a range of ink weights that covers and partly exceeds the commercial printing range at the high ink weight values, i.e. from 1 to 9 g/m2. This proved sufficient to provide useful information on the fibre removal curve that could be tested within the proposed theory.

Theory

In addition to the Stefan's law related force that acts mainly at high ink levels, it is proposed that fibre removal in the printing nip is due to two type of ink flows. A porous ink flow, penetrating the paper surface pores, and a free ink flow, at the surface of the ink-saturated surface pores. The theoretical analysis (Mangin, 1988, and Mangin, Silvy, 1990) shows that the ink flows induce sufficient drag on the fibre to overcome the bonding potential of the weakly bonded surface fibres. In the model, the structure of the paper surface is described using the Equivalent Surface Pore (Mangin, 1990b, and Mangin, Geoffroy, 1990).

The free ink film related force is expressed as:

$$F_f = \frac{4\pi(\sqrt{2}-1)V\eta}{2-\log Re}\left(\frac{h_e}{h_x}\right)^2$$

with V, the printing speed, h_e, the half thickness of the free ink film, η the viscosity of the ink during printing, h_x, the ink film thickness on the printing plate, and Re, the Reynolds number of the fluid around the fibre. Note that the Reynolds number is a function of the fibre diameter and the flow velocity around the fibre (i.e. about $dV\rho/\eta$, with d the fibre diameter and V the free ink film flow velocity).

The porous ink flow related force is expressed as:

$$F_p = \frac{\pi P \bar{\delta}^2}{8h_y\tau(2-\log Re)}$$

with P the printing pressure, δ the paper surface pore size (average value), h_y the average ink film thickness transferred to the paper, t the paper surface tortuosity, and Re the Reynolds number related to the porous flow.

A full description and derivation of the theory is given elsewhere by Mangin (1988), and Mangin and Silvy (1990).

It can be shown that the main fibre debonding force is related to the free ink film force which function is somehow an inverse function of the ink transfer function, as can be appreciated from Figures 1 and 2.

Experimental

In order to test the value of the theory to describe the fibre removal curves in the commercial printing ranges of ink weights, a series of newsprint with various combinations of thermomechanical pulp (TMP), low yield sulphite (LYS) pulp, and stone groundwood (SGWD) were manufactured on a Formette Dynamique (Dynamic Handsheet Former), then conventionally calendered at 4 smoothness

levels (i.e. 5 roughness levels as the uncalendered newsprint was included in the study). The list of furnish composition is provided in **Table 1**. The samples were then printed at 3.0, 4.6 (Scan standard), and 6.0 m/s on a GFL rotary printing press. Due to the delamination of the sheet occurring for smooth samples at high speed, some samples were printed at 5.0 m/s. Two printing pressures 3.6 MPa (low) and 5.0 MPa (high) were used. The printing inks were models inks consisting of 9 (low) and 12% (high) Picco resins in oils. Such fluids are Newtonian so the viscosity during printing can be assessed from standard rheological tests. The printing plates were phosphor bronze plates with no halftones (solid prints only). The ink weights varied between 1 and 9 g/m2. The fibres removed during printing were collected, cleaned from oil with petroleum ether then measured with a Kajaani FS100. Image analysis was also used for comparison and also for orientations studies (Mangin, 1988). An experimental design was used to decide the various levels needed to cover the study of the effects of ink weights (6), ink viscosity (2), printing speed (3), printing pressure (2), and, to a lesser extend in the scope of this article, the furnish composition (4) and paper roughness levels (5) so that 6 prints in the 1-9 g/m2 range were performed for each of the 20 samples (4 furnish x 5 roughness) in 9 printing conditions per sample

Table 1. Furnish composition

Paper/Furnish	TMP	SGWD	LYS
100 TMP	100	0	0
80 TMP	80	10	10
60 TMP	60	20	20
40 TMP	40	30	30

Results and Discussion

Effect of printing pressure

Figures 3A to **3D** present portions of the fibre removal curve within the chosen printing range (1-9 g/m2) for a 100% TMP newsprint slightly calendered (A and C) and calendered a standard smoothness level (B and D) printed at low (A and B) and high (C and D) printing speed. Each graph shows a fibre removal curve for the low (3.6 MPa) and the high (5.0 MPa) printing pressure. Similar curves are shown in **Figures 4A** to **4D** for the 40% TMP sample. It should be noted that this last sample is expected to be more resistant to fibre removal as it contains a high percentage of chemical pulp.

At a glance, it can be appreciated that the effect of pressure does not seem consistent. For Figure 3A which corresponds to a low printing speed and a rough/porous paper surface, the low printing pressure creates more lint. When the surface is closed by further calendering, the high printing pressure - as one would intuitively surmise - corresponds to the high linting situation. The effect does not occur when the printing speed is increased as can be seen from Figure 3C and 3D. With the different paper structure provided by the combination of furnishes (40% TMP, 20% SGWD, 20% LYS), the situation becomes even more complex. It should however be noted that, at low printing speed, the low printing pressure provides the highest linting situation, independently of the paper roughness. When the speed is increased, a cross-over point exists for both roughness levels. Within the frame of the proposed theory it can be deduced that

- printing pressure has an effect on the debonding energy as it controls the part of the ink film in the porous flow regime. The porous flow is defined by the porosity of the paper surface, here modified by both the calendering (surface effect) and the combination of furnishes (mass-structural effect).
- the ink film thickness participating to the porous flow controls, by difference, the ink film thickness participating to the free ink film flow (practically shear forces).
- finally, the printing speed has a direct influence on the debonding energy related to the free ink film force.

The debonding of a specific fibre is the result of previous interactions combined with the bonding potential of the furnish used to manufacture the papers. This could be further explained using the force equations related to the ink flows.

The porous flow force being proportional to the pressure times the porosity squared divided by the thickness of the ink film transferred to the paper, the question is to calculate which condition, as expressed below, will create a situation where the force related to a low printing pressure will be greater than that of the high pressure.

$$F_p \propto \frac{P\bar{\delta}^2}{h_y} \Rightarrow F_{LP} \geq F_{HP}$$

The situation can occur if the ink film transferred at low printing pressure y_{LP}, for a given ink weight on the printing plate is lower than that transferred at high pressure y_{HP} - which is usually the case - with a ratio of printing pressure that favours the ratio of corresponding ink weights. This is bound to occur at low printing speeds and rough/porous surfaces (Figure 3A) while the porous flow is limited when the surface is closed (Figure 3B). A higher printing speed does not favour flow in the porous medium due to the reduced contact time in the printing

nip. Everything else being kept constant, when the pressure increases, the force related to the porous flow, directly proportional to the pressure, increases.

Furthermore, the free ink film force is proportional to the square of a factor expressed as 1 minus the fractional ink transfer.

$$F_l \propto \frac{1}{2}\left(1 - \frac{h_y}{h_x}\right)^2$$

Ink transfer is higher for the high pressure, i.e. when pressure increases h_y increases while, as seen above, the force related to the porous flow increases too. However, we also have

$$1 - \frac{h_y}{h_x} \downarrow \Rightarrow F_l \downarrow$$

i.e. the force related to the free ink film flow decreases with increasing printing pressure. Approximate evaluation of the forces involved (Mangin, 1988) thus explain the cross-over point situation in Figures 4C and 4D.

The fibre removal curves for the 80% and 60% TMP samples not shown here have intermediate shapes with similar behaviour.

Effect of printing speed

Figures 5A to 5D present portions of the fibre removal curve within the chosen printing range (1-9 g/m2) for a 100% TMP newsprint at increasing smoothness levels (from A to D) printed at low (3.6 MPa) printing pressure. Each graph shows a fibre removal curve for the 3 printing speeds, i.e. low (3.0), medium (4.0 or 4.6) and high (5.0 or 6.0) printing speeds. Similar curves are shown in **Figures 6A to 6D** for the 40% TMP sample to illustrate that the effects shown are similar while occurring at a lesser extent. For the two types of ink flows, the effect of the printing speed on the debonding of fibres is linked to the relative importance of the two flows. Besides the speed which either enhances (low level) or reduces (high level) the porous flow, the importance is here based on the force related to the free ink flow. The porous flow is preponderant for the porous structure (low calendering level) up to a saturation point in ink which explain the cross-over point in the fibre removal curves seen for both the 100% TMP and 40% TMP at low calendering level. The differences among the 3 printing speeds become minor at higher calendering level when the surface is closed. Here, calculations of force values indicated marginal differences in the forces levels. The same was true for the 80% and 60% TMP samples.

Effect of ink viscosity

Figures 7A to **7D** present the fibre removal curve in the 1-9 g/m2 range for the 100% TMP sample printed at low printing pressure (3.6 MPa). Low printing speed corresponds to the Figures 7A and 7B, while high printing speed corresponds to Figures 7C and 7D. The open rough surfaces correspond to Figures 7A and 7C while the closed smooth surfaces correspond to Figures 7B and 7D. Similar fibre removal curves are shown for the 40% TMP sample in **Figures 8A** to **8D**. Each Figure include the fibre removal curve at low in viscosity (9% resins) and high viscosity (12% resins). In these model experiments performed to illustrate applications of the linting mechanisms theory, the liquids are Newtonian.

The curves are chosen to illustrate that all configurations are possible as all 3 forces should be considered to explain each data point. Following equations of proportionality should then be considered

F(due to ink film splitting) $\propto V\eta$ (see Mangin, Silvy, De Grâce 1990)

$F_p \propto (h_y \text{ Log } \eta)^{-1}$

$F_l \propto \eta(\text{Log } \eta)^{-1}$

As was discussed for the effect of printing pressure, the viscosity has a direct effect on the ink flow within the porous structure. The speed of the ink flow within the porous structure decreases as the viscosity increases. The debonding theory predicts that effects are opposite to that of the printing pressure. A higher pressure induces a higher debonding of the surface fibres while a higher viscosity induces a reduction in the ink flow speed. This in turns amounts to lower shear rate at the paper surface and a lower debonding. Practically, a high viscosity ink reduces ink penetration in the porous medium and the porous ink flow speed. Calculations shows that with identical paper porosity, ink transfer, and printing pressure, the debonding forces related to the two viscosity have very similar values. At low printing speed, if the paper surface structure is open and porous, the low viscosity ink favours saturation of the porous medium at low ink weights. The average porous flow speed thus decreases and therefore its debonding potential (Figure 7A). At high ink levels, the effect of viscosity is reversed as at these levels the free ink film thickness is higher and its debonding potential the main factor for fibre removal: i.e. a higher fibre removal at high ink weights as seen in Figure 7A.

At high printing speed, the predominant factors are shear forces in the free ink film and even tack forces. As previously, a low viscosity favours ink penetration (porous flow force) which results in a higher debonding potential for the low viscosity. As tack forces are concerned, it should be pointed out that with similar chemical structures - as is the case here - tack forces are related to viscosity. For the 40% TMP sample, in most cases a higher viscosity equates to a higher debonding and a higher fibre removal. Figure 8B has a specific interest as

combination of forces induces similar fibre removal curves for low and high viscosity inks.

Conclusions

The mechanism of fibre removal in a printing nip is based on the interaction of 3 forces, two based on ink flow (free and porous), and ink film splitting force (sometimes called "tack"). As the ink flows have different interactions with various paper surface structures and as the ration of porous versus free ink film flow varies as an interaction of both printing parameters such as printing speed, printing pressure, and ink viscosity, and paper parameters such as surface porosity and ink transfer, the linting situation is necessarily a complex interactive phenomena. It should also be stressed that ink transfer, a parameter within the force equations derived, also relates from the interaction between paper and printing conditions.

It should also be stressed that an increase in ink viscosity, printing speed, and printing pressure does not necessarily induces an increases in linting as the combination of the forces can produce reverse effects.

Finally, the new model proposed to explain the linting mechanisms was found very useful to elucidate these complex interactions as each condition of linting, when both printing conditions and paper properties are known, can be calculated.

Literature Cited

Mangin, Patrice J.

1987 A review of the evaluation of the offset linting propensity of paper, TAGA Proceedings, 397-442

1988 Etude de la déstructuration de la surface du papier en zone d'impression offset, PhD Thesis, Institut National Polytechnique de Grenoble, Grenoble, France (in French).

1990a Offset linting studies. Part I - A critical review of the effects of printing parameters on the linting propensity of paper, CPPA/TS Annual Meeting, Preprints B143-B154, and

1990b The measurement of paper roughness - A 3D profilometry approach, Advances in Printing Science and Technology, W.H. Banks Ed., Pentech Press, London, Vol.20, 218-235.

1991 A critical review of the effects of printing parameters on the linting propensity of paper, Journal of Pulp and Paper science, Vol.17, no.5, J156-J163.

Mangin, Patrice J. and Geoffroy, Philippe
1990 Printing roughness and compressibility: a novel approach based on ink transfer, Advances in Printing Science and Technology, W.H. Banks Ed., Pentech Press, London, Vol.20, 249-265.

Mangin Patrice J., and Silvy Jacques
1990 Surface pore structure, ink flow, and fibre removal during printing, International Paper Physics Seminar, Kalamazoo, MI, USA (abstract only).

Mangin, Patrice J., Silvy, J., and De Grâce, J.H.
1990 Offset linting studies. Part 2 - Further contribution to linting theories, 6th International Printing and Graphic Arts Conference, Vancouver, B.C., Can., Proceedings 109-119.

Oittinen, Pirkko
1976 Fundamental rheological properties and tack of printing inks and their influence on ink behaviour in a printing nip, PhD Thesis, Acta Polytechnica Scandinavia, Ch.131, 79, Helsinki University of Technology, Otaniemi, Finland.

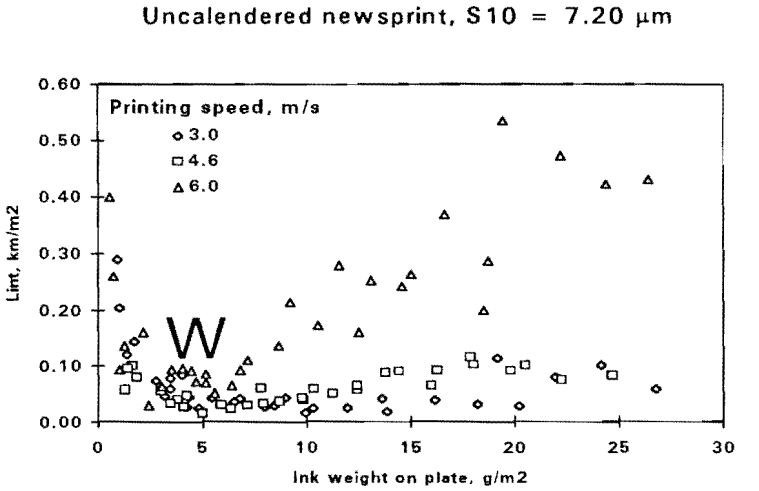

Figure 1. Lint removed from an un-calendered newsprint printed at 3.0, 4.6, and 6.0 m/s. The fibre removal curve shows the complexity of the phenomena with a typical W-shape at commercial printing ranges.

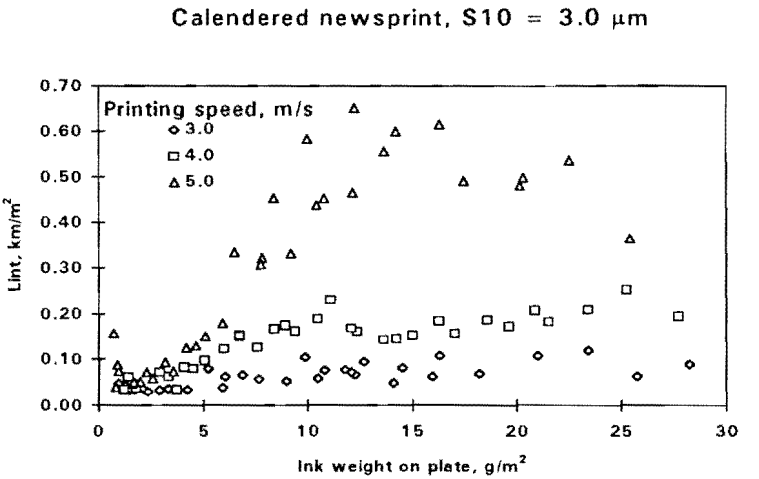

Figure 2. Lint removed from a calendered newsprint printed at 3.0, 4.0, and 5.0 m/s. Delamination occurred at 6.0 m/s. The decrease of lint, as predicted by a decrease in Stefan's law related-force, only occurs after saturation of the fibre network, i.e. around 15 g/m^2.

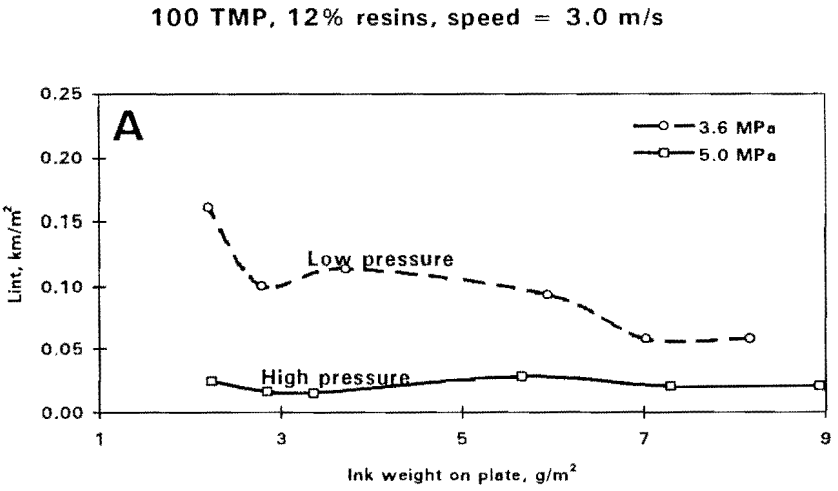

Figure 3A. Effect of printing pressure for a 100% TMP newsprint printed at 3.0 m/s with a model ink made of 12% Picco resins in mineral oil. Newsprint, slightly calendered has a Parker Print-Surf roughness S10 of 6.25 μm.

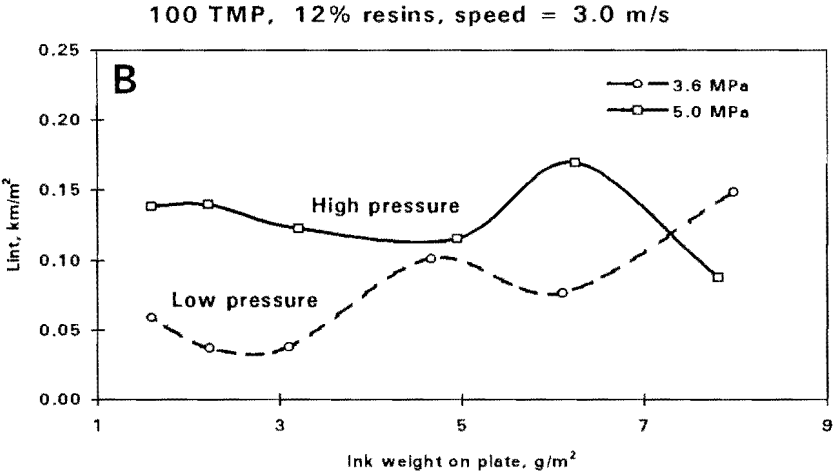

Figure 3B. Effect of printing pressure for a 100% TMP newsprint printed at 3.0 m/s with a model ink made of 12% Picco resins in mineral oil. Newsprint is here calendered at a Parker Print-Surf roughness S10 of 3.50 μm.

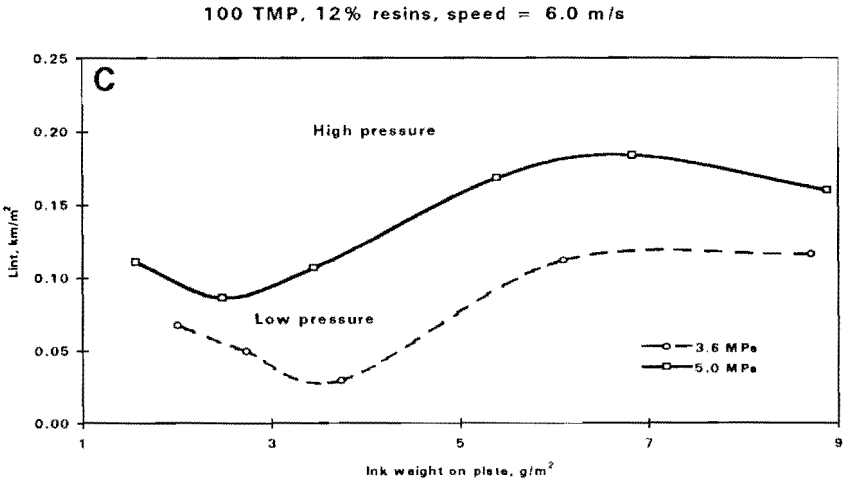

Figure 3C. Effect of printing pressure for a 100% TMP newsprint printed at 6.0 m/s with a model ink made of 12% Picco resins in mineral oil. Newsprint, slightly calendered has a Parker Print-Surf roughness S10 of 6.25 μm.

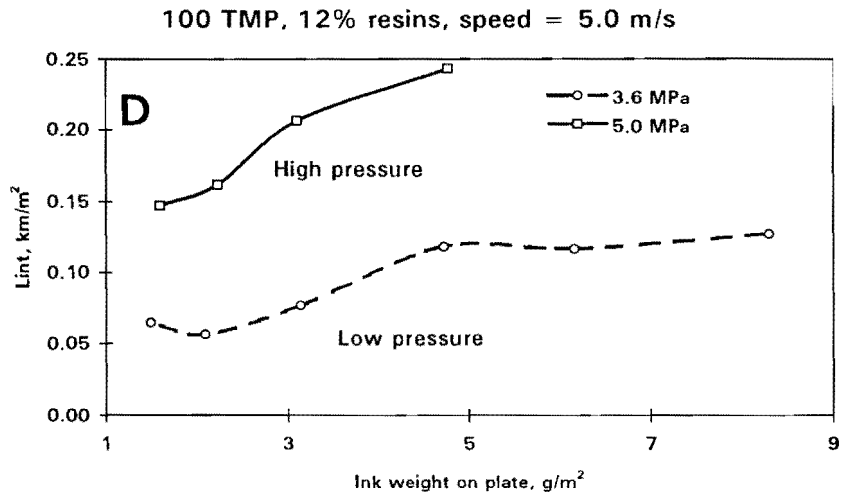

Figure 3D. Effect of printing pressure for a 100% TMP newsprint printed at 5.0 m/s with a model ink made of 12% Picco resins in mineral oil. Newsprint is here calendered at a Parker Print-Surf roughness S10 of 3.50 μm. Note that delamination occurred at 6.0 m/s.

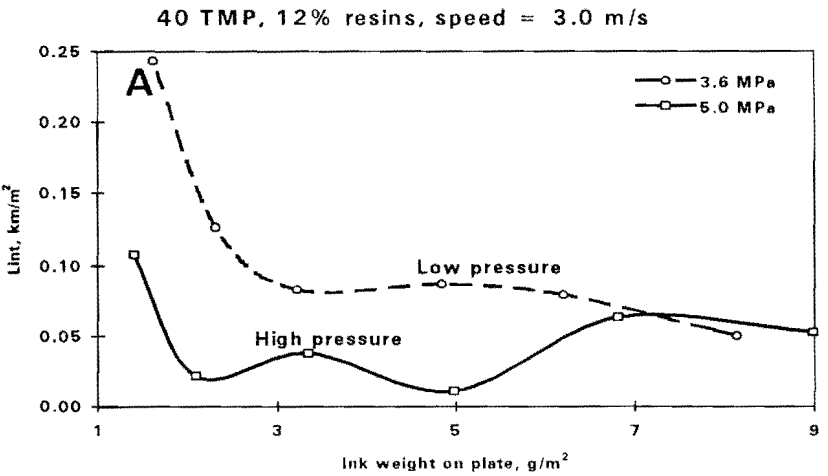

Figure 4A. Effect of printing pressure for a 40% TMP newsprint printed at 3.0 m/s with a model ink made of 12% Picco resins in mineral oil. Newsprint, slightly calendered has a Parker Print-Surf roughness S10 of 6.15 μm.

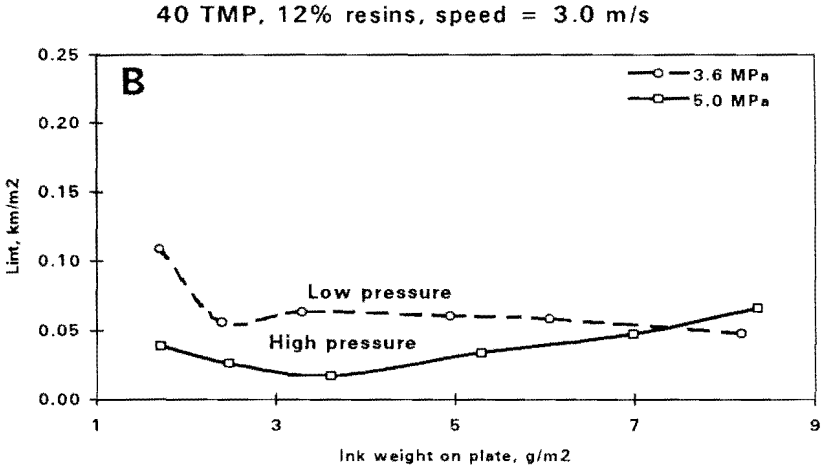

Figure 4B. Effect of printing pressure for a 40% TMP newsprint printed at 3.0 m/s with a model ink made of 12% Picco resins in mineral oil. Newsprint is here calendered at a Parker Print-Surf roughness S10 of 3.60 μm.

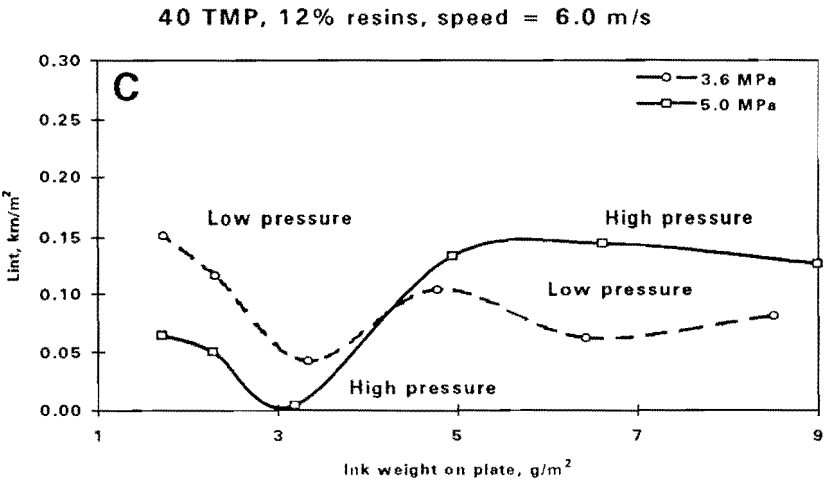

Figure 4C. Effect of printing pressure for a 40% TMP newsprint printed at 6.0 m/s with a model ink made of 12% Picco resins in mineral oil. Newsprint, slightly calendered has a Parker Print-Surf roughness S10 of 6.25 μm.

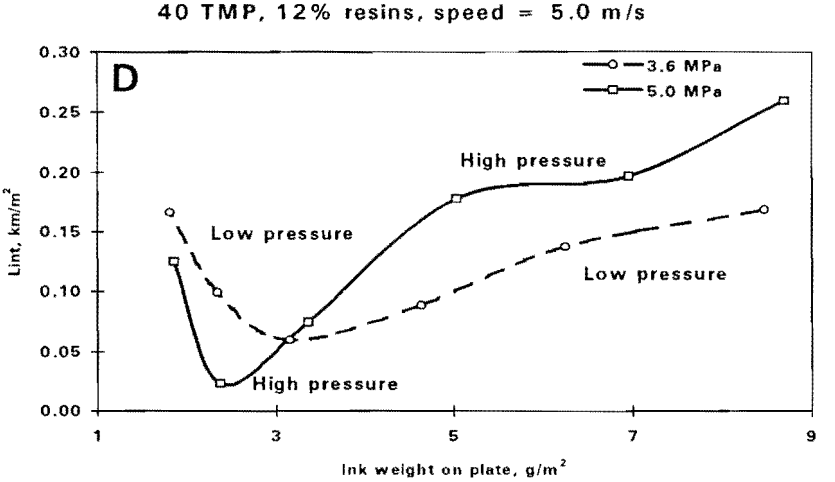

Figure 4D. Effect of printing pressure for a 40% TMP newsprint printed at 5.0 m/s with a model ink made of 12% Picco resins in mineral oil. Newsprint is here calendered at a Parker Print-Surf roughness S10 of 3.50 μm. Note that delamination occurred at 6.0 m/s.

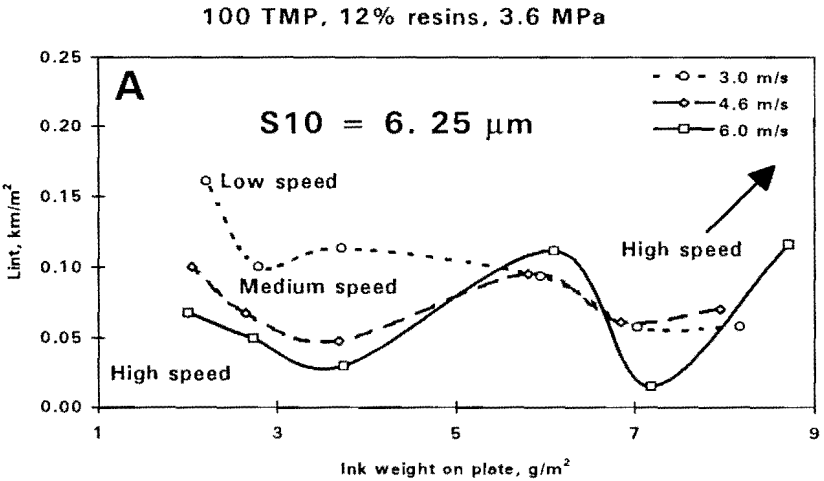

Figure 5A. Effect of printing speed for a 100% TMP newsprint printed at 3.6 MPa with a model ink made of 12% Picco resins in mineral oil. PPS roughness S10 is 6.25µm.

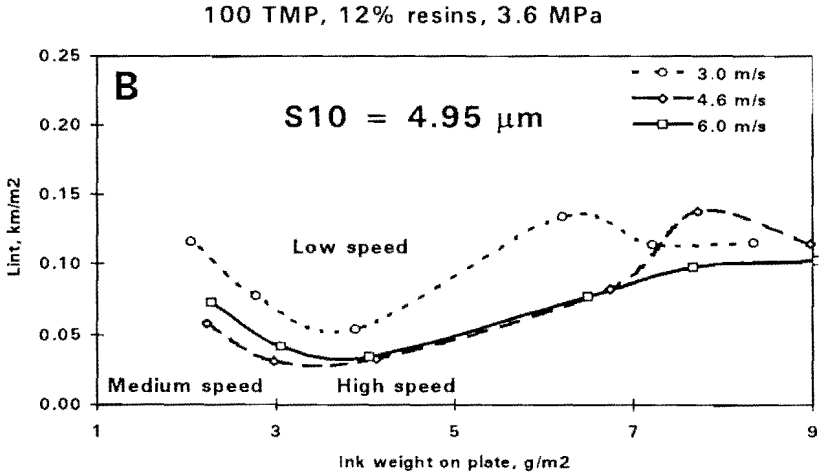

Figure 5B. Effect of printing speed for a 100% TMP newsprint printed at 3.6 MPa with a model ink made of 12% Picco resins in mineral oil. PPS roughness S10 is 4.95µm.

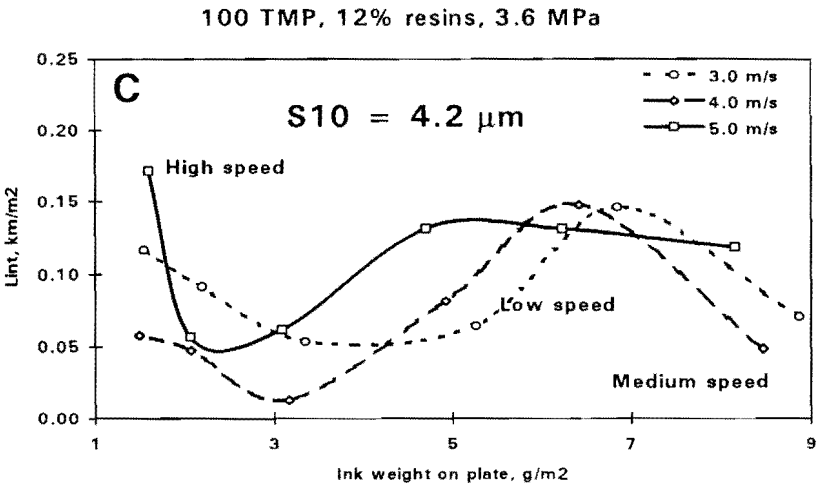

Figure 5C. Effect of printing speed for a 100% TMP newsprint printed at 3.6 MPa with a model ink made of 12% Picco resins in mineral oil. PPS roughness S10 is 4.20µm.

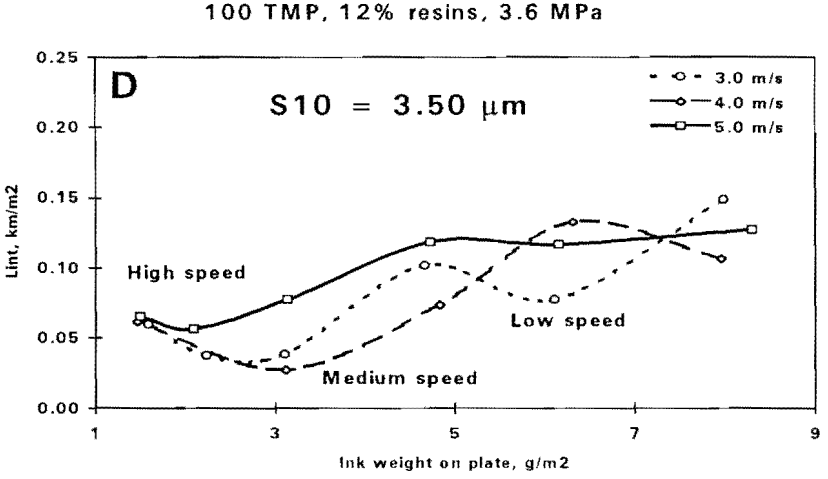

Figure 5D. Effect of printing speed for a 100% TMP newsprint printed at 3.6 MPa with a model ink made of 12% Picco resins in mineral oil. PPS roughness S10 is 3.50µm.

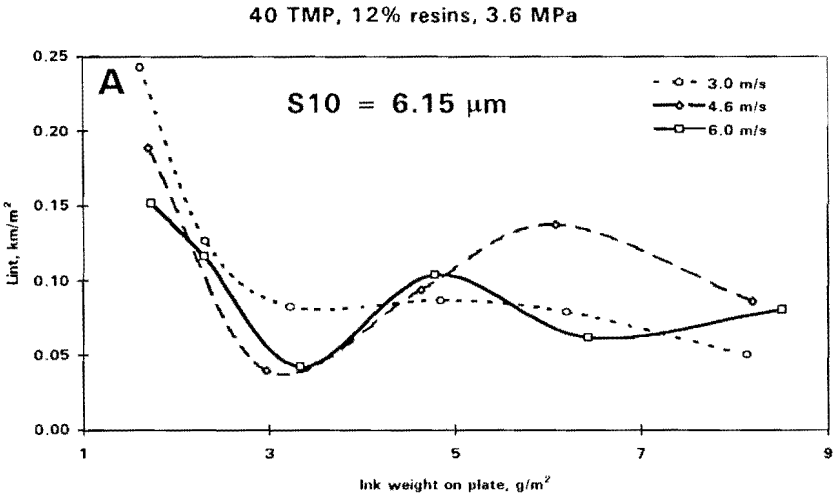

Figure 6A. Effect of printing speed for a 40% TMP newsprint printed at 3.6 MPa with a model ink made of 12% Picco resins in mineral oil. PPS roughness S10 is 6.15µm.

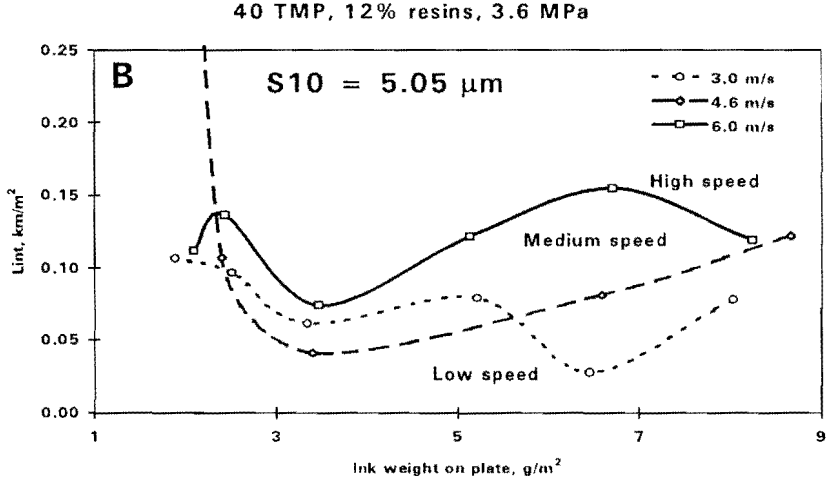

Figure 6B. Effect of printing speed for a 40% TMP newsprint printed at 3.6 MPa with a model ink made of 12% Picco resins in mineral oil. PPS roughness S10 is 5.05µm.

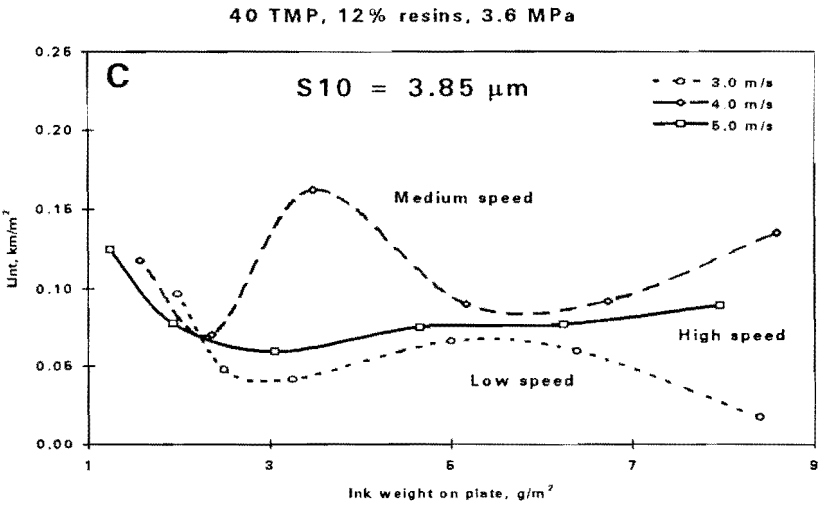

Figure 6C. Effect of printing speed for a 40% TMP newsprint printed at 3.6 MPa with a model ink made of 12% Picco resins in mineral oil. PPS roughness S10 is 3.85µm.

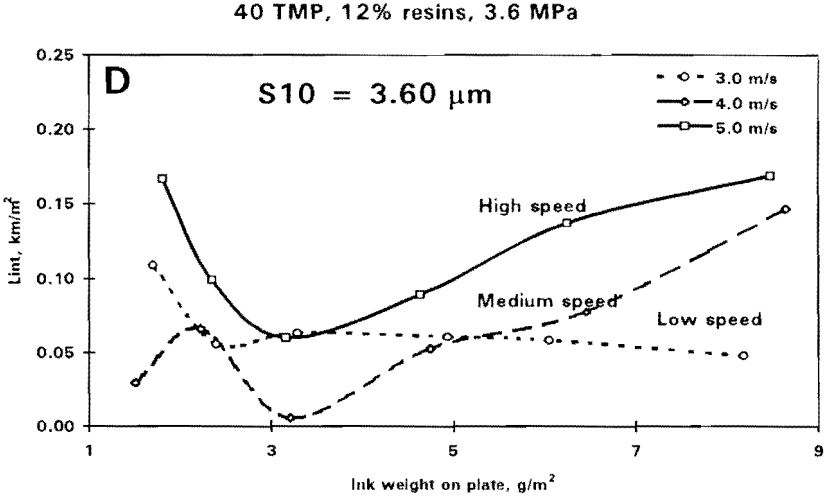

Figure 6D. Effect of printing speed for a 40% TMP newsprint printed at 3.6 MPa with a model ink made of 12% Picco resins in mineral oil. PPS roughness S10 is 3.60µm.

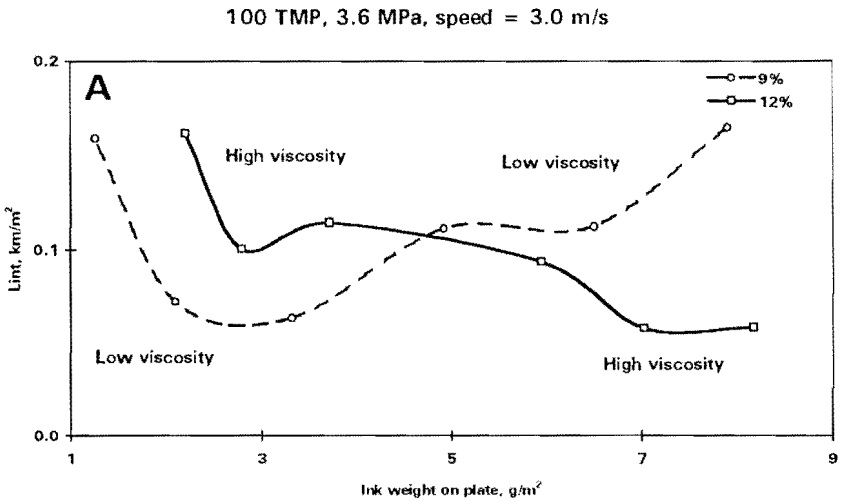

Figure 7A. Effect of viscosity for a 100% TMP newsprint printed at 3.6 MPa with model inks made of 9 and 12% Picco resins in mineral oil. PPS roughness S10 is 6.25μm, printing speed is 3.0 m/s.

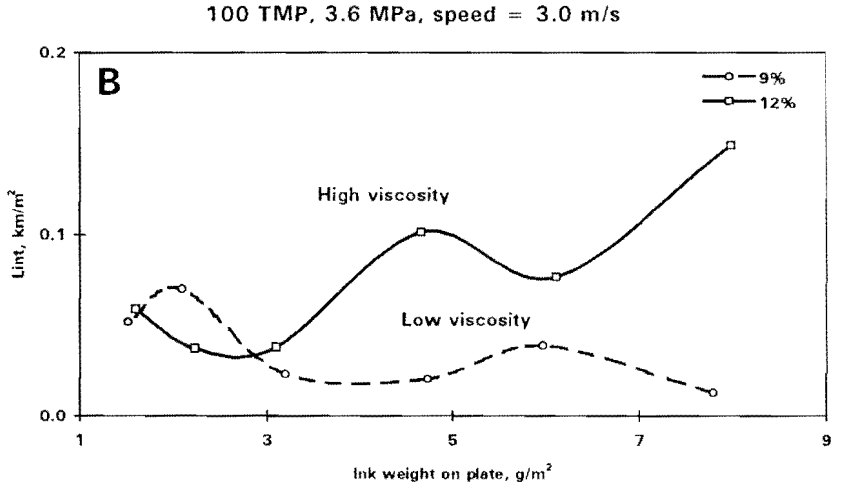

Figure 7B. Effect of viscosity for a 100% TMP newsprint printed at 3.6 MPa with model inks made of 9 and 12% Picco resins in mineral oil. PPS roughness S10 is 3.50μm, printing speed is 3.0 m/s.

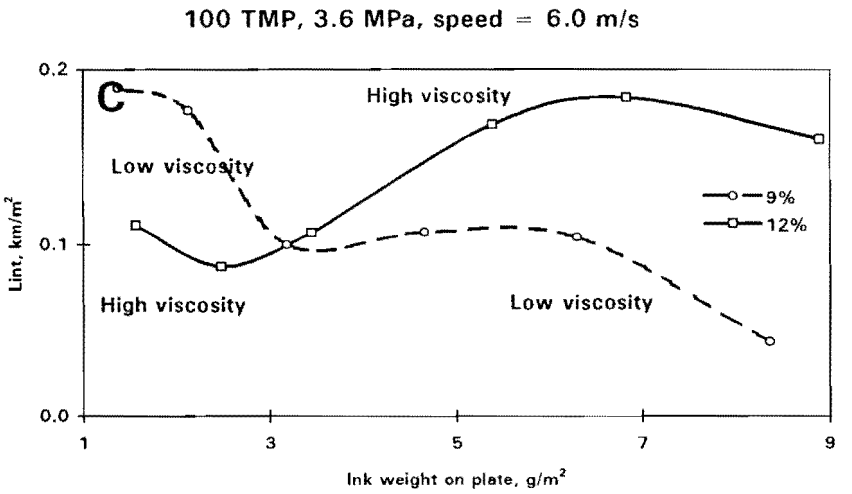

Figure 7C. Effect of viscosity for a 100% TMP newsprint printed at 3.6 MPa with model inks made of 9 and 12% Picco resins in mineral oil. PPS roughness S10 is 6.25μm, printing speed is 6.0 m/s.

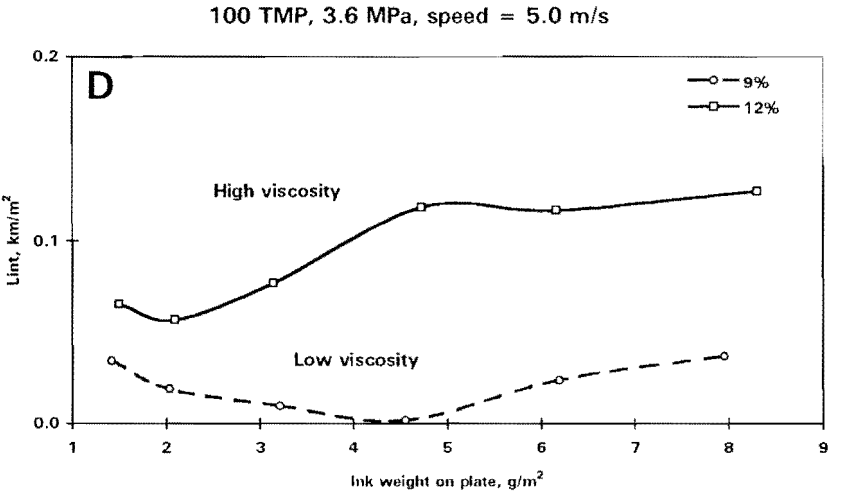

Figure 7D. Effect of viscosity for a 100% TMP newsprint printed at 3.6 MPa with model inks made of 9 and 12% Picco resins in mineral oil. PPS roughness S10 is 3.50μm, printing speed is 5.0 m/s. Delamination occurred at 6.0 m/s.

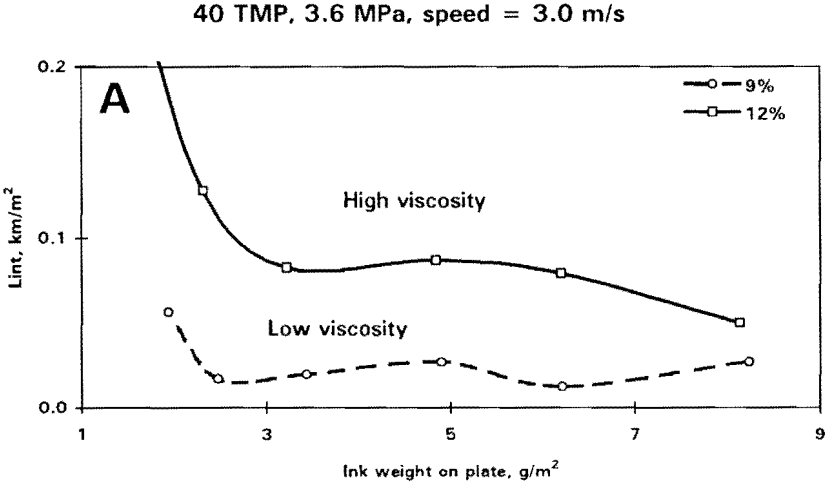

Figure 8A. Effect of viscosity for a 40% TMP newsprint printed at 3.6 MPa with model inks made of 9 and 12% Picco resins in mineral oil. PPS roughness S10 is 6.15μm, printing speed is 3.0 m/s.

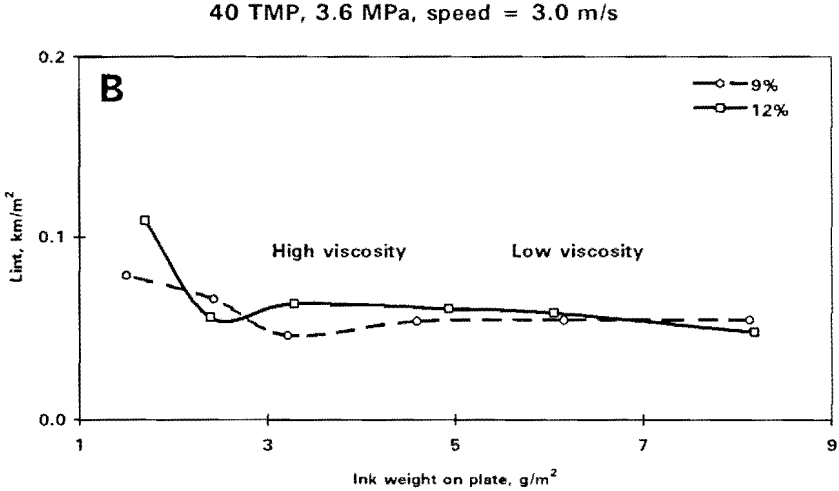

Figure 8B. Effect of viscosity for a 40% TMP newsprint printed at 3.6 MPa with model inks made of 9 and 12% Picco resins in mineral oil. PPS roughness S10 is 3.60μm, printing speed is 3.0 m/s.

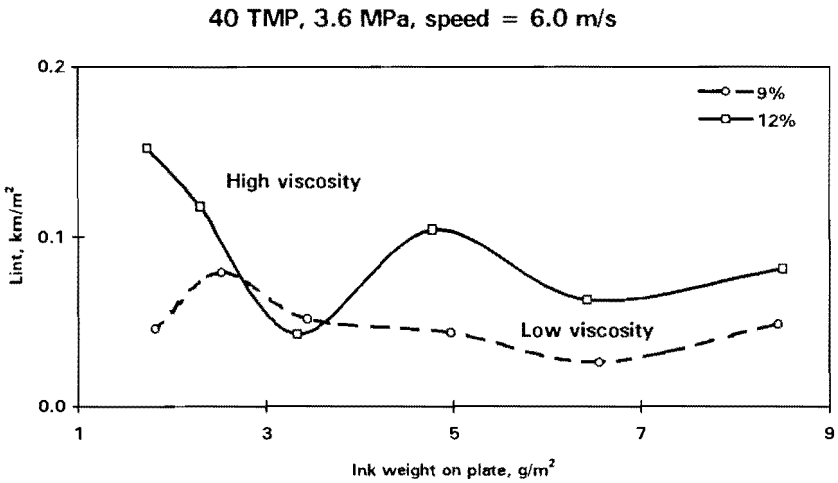

Figure 8C. Effect of viscosity for a 40% TMP newsprint printed at 3.6 MPa with model inks made of 9 and 12% Picco resins in mineral oil. PPS roughness S10 is 6.15μm, printing speed is 6.0 m/s.

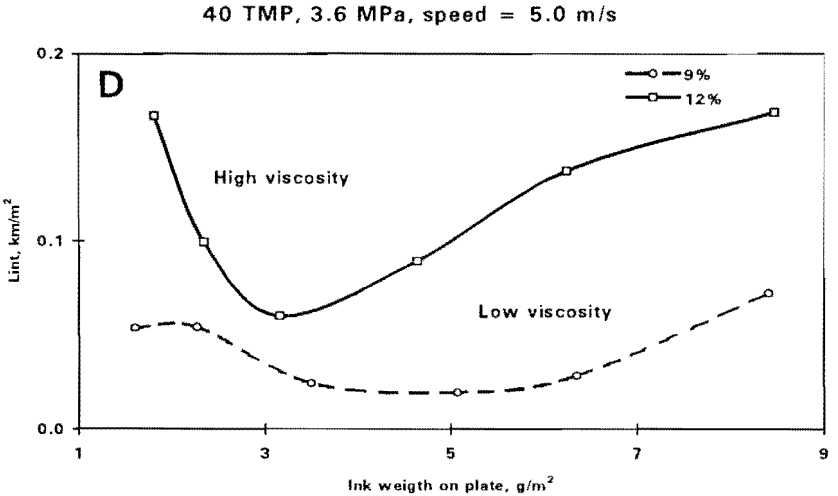

Figure 8D. Effect of viscosity for a 40% TMP newsprint printed at 3.6 MPa with model inks made of 9 and 12% Picco resins in mineral oil. PPS roughness S10 is 3.60μm, printing speed is 5.0 m/s. Delamination occurred at 6.0 m/s.